

Lab on a Chip

Accepted Manuscript



This is an *Accepted Manuscript*, which has been through the Royal Society of Chemistry peer review process and has been accepted for publication.

Accepted Manuscripts are published online shortly after acceptance, before technical editing, formatting and proof reading. Using this free service, authors can make their results available to the community, in citable form, before we publish the edited article. We will replace this *Accepted Manuscript* with the edited and formatted *Advance Article* as soon as it is available.

You can find more information about *Accepted Manuscripts* in the [Information for Authors](#).

Please note that technical editing may introduce minor changes to the text and/or graphics, which may alter content. The journal's standard [Terms & Conditions](#) and the [Ethical guidelines](#) still apply. In no event shall the Royal Society of Chemistry be held responsible for any errors or omissions in this *Accepted Manuscript* or any consequences arising from the use of any information it contains.

ARTICLE

Origami Paper-Based Fluidic Batteries for Portable Electrophoretic Devices

Cite this: DOI: 10.1039/x0xx00000x

Sung-Sheng Chen,^a Chih-Wei Hu,^b I-Fan Yu,^a Ying-Chih Liao,^{b*} Jing-Tang Yang^{a*}

Received 00th January 2012,
Accepted 00th January 2012

DOI: 10.1039/x0xx00000x

www.rsc.org/

A manufacturing approach for paper-based fluidic batteries was developed based on the origami principle (three-dimension paper folding). Microfluidic channels were first created on filter paper with a wax-printing method. Copper and aluminium sheets were then glued onto the paper as electrodes for the redox reaction. After the addition of copper sulphate and aluminium chloride, commonly available cellophane paper was attached as a membrane to separate the two electrodes. The resulting planar paper sheets were then folded into three-dimensional structures and compiled as a single battery with glue. The two half reactions (Al/Al^{3+} and Cu/Cu^{2+}) in the folded batteries provided a real potential from 0.82 V (one cell) to 5.0 V (eight cells in series) depending on the origami designs. The prepared battery can provide a stable current 500 μA and can light a regular LED for more than 65 min. These paper-based fluidic batteries in a set can also be compiled into a portable power bank to provide electric power for many electric or biomedical applications, such as LED lights and electrophoretic devices, as we report here.

Introduction

Paper-based devices (PAD) attract widespread attention for their small cost, flexible property, rapid production, and ease of integration with other fluidic or analytical devices. Many paper-based devices were developed for various fields, such as all-polymer batteries,^{1, 2} supercapacitors,^{3, 4} metal-polymer batteries,⁵ electrochemical sensors⁶ and microfluidic devices for bioanalysis.^{7,8} In all cases, the development of paper-based batteries is an important factor for these new devices. The concerns of cost, performance and toxicity pertinent to these paper-based batteries become a huge advantage for use in resource-limited areas in the world to provide a stable electronic platform for separations, concentration and electrochemical analysis.

A most essential component in a PAD is a microfluidic channel, which directs the motion of test fluids in the paper. Pioneers have designed various ways to create hydrophilic or hydrophobic patterns on papers. Martinez et al.⁹⁻¹¹ first used photolithography to create microfluidic channels on paper. Moreover, by stacking multilayers of planar microfluidic channels, they demonstrated that a three-dimensional (3D) microfluidic structure can be assembled.¹² Although this photolithography technique is successful and produces high-resolution microfluidic channels ($\sim 200 \mu\text{m}$), expensive photomasks and instruments are needed for their micro-fabrication. To decrease the costs, Bruzewicz et al.¹³ used an inkjet printer to deposit polymeric ink on papers to generate microfluidic channels, and showed well the twist resistance and flexible ability of the printed microfluidic channels. Dungchai et al. subsequently proposed a cheap screen-printing method

with melting wax to create micro-patterns rapidly on paper.¹⁴ Nilghaz et al. extended the same skill to produce fluidic channels on cloth.¹⁵ To avoid the mask preparation in the screening-printing method, Carrilho et al.¹⁶ utilized a computerized wax printer to make microfluidic channels on paper with a feature size about 300 μm . This wax-printer technique has been extensively applied in the literature because of its great flexibility in microfluidic design changes.

Origami, a traditional art of paper folding from Japan, has recently become widely applied in making 3D PAD for diverse purposes. The principle of origami is to use a single paper to construct a stereo object from a flat sheet. The folded 3D PAD from origami have been shown to be useful in chemical analysis, such as colorimetry and fluorescence,^{17,18,19} DNA extraction²⁰ and chemiluminescent markers.^{21,22} In contrast to the aforementioned paper-stacking methods, origami methods possess characteristics of ease of handling and rapid assembly for manufacturing 3D PAD. Origami skills have thus been widely used to integrate various paper-based fluidic devices, and have shown a great potential in simplifying the fabrication of paper-based devices.

Self-powered PAD have also been a trend to advance the portability and to extend the PAD applications in many analytical devices. With the electric power from an on-chip device, one can easily observe or analyse chemical reactions on site without bulky external power supplies. Thom et al. fabricated fluidic batteries by stacking multi-layer 2-D microfluidic channels into a 3-D structure.^{23,24} The battery contained two metal electrodes separated with a salt bridge, and could power an LED light for about 20 min. Zhang et al. subsequently showed self-powered electrochemiluminescent biosensing devices fabricated with origami skill with an on-chip

battery.²⁵ Although previous work showed the great potential of fluidic batteries in self-powered PAD devices, the assembly was either cumbersome or involved clamping fixtures. A systematic investigation regarding a simplified fabrication is thus needed to explore the possibility of applying the origami skills in fabricating a fluidic battery.

In this work, we developed a new method to make a paper-based fluidic battery on combining a wax-printing method and origami skills. The on-chip batteries can be connected in series or in parallel to obtain a large open-circuit voltage and a stable output current. These paper-based fluidic batteries in a set can also be compiled into a portable power bank to provide electric power of several milliwatts for many electric or biomedical applications. To demonstrate the possibility of self-powered paper-based devices for inexpensive separation of chemicals, a miniaturized electrophoretic device with low power requirements, instead of regular electrophoretic devices with bulky external power supplies, will also be fabricated and tested.

Experiments

Materials and Chemicals

Deionized water (18.2 M Ω -cm at 25 °C, SMART DQ-3, Sun-Great Technology Co., Ltd.), copper tape (width 5 mm, thickness 0.066 mm, product #1181, 3M) and red LED (SML-211UT) (Weltrend Semiconductor, Inc.) were obtained from the indicated sources. CuSO₄ (99.0 %, Sigma-Aldrich[®]) and AlCl₃ (99.5 %, Nihon Shiyaku Reagent) were all used as received without purification. Cellophane, Al foil (99 %, thickness 0.2 mm) and Cu foil (99%, thickness 0.2 mm), without purification, were purchased from a local shop.

Fabrication

All layouts for the microfluidic channels were designed with software (AutoCAD[®]), and were printed on filter papers (Advantec No. 1) with a wax printer (Fuji Xerox 8570), as described by Matinez et al.⁹ Here, No. 1 filter papers from Advantec were used to assembly the batteries for their fast water absorption and quick chemical transport rates. The printed papers were then heated at 150 °C for 90 s on a hotplate to form well circumscribed microfluidic channels. Fluidic batteries in five layouts, which correspond to one-cell, two-cell, four-cell, six-cell and eight-cell fluidic batteries, respectively, are shown in Fig. S1. Each fluidic battery comprised several layers that are differentiable into four types: water inlet, water-transfer channels, electrolyte layers and electrodes. The number of total layers depends on the number of cells in the battery and the linkage of cells in series or parallel.

Figure 1(a) shows an exemplary design of the origami fluidic batteries. The sequence of production involves folding and assembling five pieces of patterned papers: a water-inlet layer (layer 1), a water-transfer layer (layer 2), two electrolyte layers (layers 3 and 4) and the electrode layer (layer 5). After the 2-D fluidic channels were fabricated, first AlCl₃ (10 μ L, 0.67 M) and CuSO₄ (10 μ L, 1 M) aqueous solutions were dripped separately into the electrolyte channels, with drying in an oven at 50 °C for 15 min. Next, a cellophane film (area 10 \times 15 mm²) was glued on layer 4 (step 2 in Fig. 1 (a)). After that, layers 1 to 4 were glued together as shown in steps 3-5. Double side tapes were then pasted on layer 5; Cu and Al metal foils (areas 5 \times 25 mm²) were attached to the tapes. Finally, the electrode layer was stacked to form a fluidic battery. Oblique

and side views of the fluidic battery are presented in Fig. 1 (b) and (c).

The fabrication of a multiple-cell battery is similar to that of the one-cell battery. The layouts of multiple-cell fluidic batteries and folding processes are presented in Fig. S4 to S7 in Electronic Supplementary Information (ESI).

Electrical measurements

With a potentiostat (Gamry reference 6000) we measured the closed-circuit current I_{SC} and open-circuit voltage V_{OC} to estimate the power of the fluidic batteries. Deionized water (30 μ L) was dripped into the inlet hole in the dry fluidic battery. I_{SC} or V_{OC} measurements began immediately after the addition of water and continued for at least 20 min.

To estimate the duration of the prepared fluidic batteries, we wired an LED lamp to the batteries with alligator clamps. Because the forward voltage of the LED is 1.8 V, three one-cell batteries in series or a battery with four cells in series was used to provide power to the LED. During observation of the LED lighting, we added \sim 10 μ L water every 20 min during the experiment to prevent the batteries from drying or losing power.

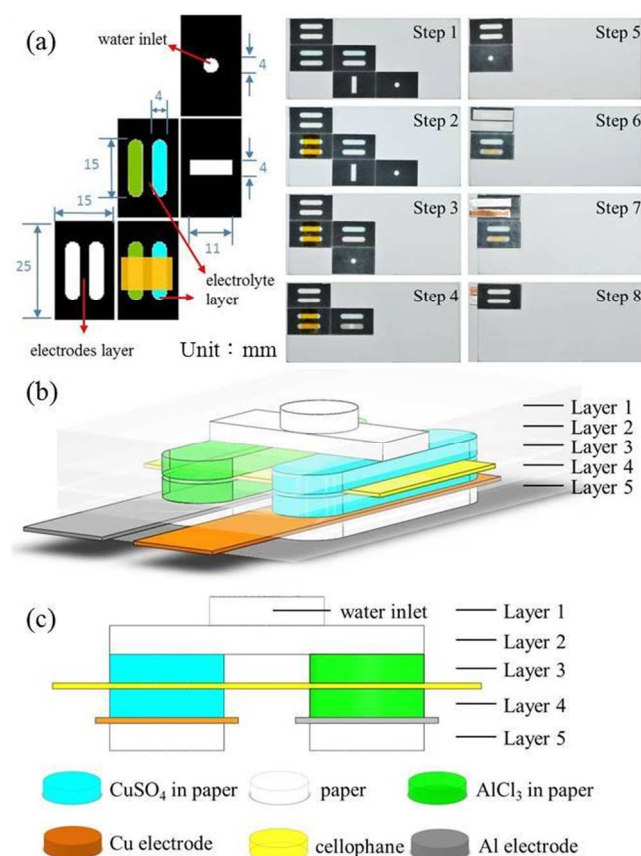


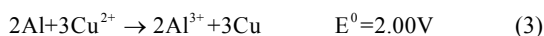
Fig. 1 (a) Planar layout and folding sequence of a single-cell fluidic battery. (b) 3-D oblique view of the one-cell fluidic battery. (c) Side view of the one-cell fluidic battery. Layer 1 and 2 are fluidic channels to introduce water into the battery. In layer 3 and layer 4, CuSO₄ and AlCl₃ are deposited in the paper and serve as electrolytes. A piece of cellophane film is attached between layer 3 and layer 4 to connect the two electrolyte channels for ion exchange. The Cu and Al films located between layer 4 and 5 serve as electrodes.

Results and Discussion

With our origami designs, as shown in Fig. 1, the printed 2D channels are easily assembled into 3D structures. Galvanic cells of varied number can be made and linked in parallel or in series in one battery. Basic electric characteristics, such as open-circuit voltage, V_{OC} , and closed-circuit current I_{SC} , of the fluidic batteries are tested to assess the performance of the fluidic batteries. Related factors or design parameters affecting the electric performance of the batteries are also discussed to optimize the battery designs. Various origami designs of similar principle are presented to show the capability of this technique for rapid production of fluidic batteries. A packaging was developed to seal the battery so that it can be soaked partly in water for prolonged usage without manual addition of water as in previous work. In two further sessions, electric devices, such as LED and electrophoretic device, are connected to the battery to show practical applications of a fluidic battery for analytical devices.

(a) Factors regarding open circuit voltage (V_{OC})

For comparison with the silver-aluminium batteries used in the literature, copper and aluminium were chosen as the galvanic metal electrodes in this work as they are cheap and commonly available. The half reactions of Al/Al^{3+} , Cu/Cu^{2+} and total reaction are shown in Eq. (1) ~ (3) with the standard electric potentials.



Although the overall standard electric potential is slightly smaller than that of Ag/Al (2.46 V), the copper salts and metal sheets are both much cheaper than silver and can still provide a satisfactory electric potential. Moreover, the copper ion, which is the limiting reagent in the redox reaction, can transfer two electrons in this galvanic battery, twice of the Ag ions used in the literature. The batteries can hence theoretically provide more electric capacity with the same molar amount added. In a one-cell system, the battery provides a $V_{OC} = 0.82 \text{ V}$. Relative to the ideal reaction of an Al/Cu battery, the relative voltage decrease is about 59 % ($2.00 \rightarrow 0.82 \text{ V}$), similar to the decreased V_{OC} in the literature ($2.46 \rightarrow 1.30 \text{ V}$, 53 % loss in reference 23). Although the internal resistance of a cellophane film is potentially smaller than a paper-type salt-bridge battery, the active electrode area in this work is 5 times as large as those in reference 23 ($15 \times 4 \text{ mm}^2$ vs. $7.9 \times 1.5 \text{ mm}^2$). The large sheet resistance and/or overall impedance can thus result in a more severely decreased V_{OC} . The larger active area with a cellophane film as separation layer also helps the battery to provide a steady V_{OC} output for at least 20 min (shown later in Fig. 3), which is much better than the paper-based batteries in the literature.

(b) Closed circuit current (I_{SC})

The closed-circuit current (I_{SC}) of batteries is related to the concentration of reactants (Al and Cu^{2+}), active areas of the electrodes, and the rate of ionic exchange between electrodes. In this work, we introduced cellophane film as a separation layer or ion-exchange medium to simplify the cumbersome salt-bridge assembly. Because the ionic exchange involves the passage of water through the cellophane, pore structures in cellophane films can significantly affect the ion-exchange efficiency, i.e., values of I_{SC} . Water-soaked cellophane films

generally have swollen or loose fibre structures and thus possess superior wettability to pass water. To enhance the rates of ion exchange, pre-wetting was used in this work. The cellophane film was soaked in deionized water for 5 min and dried in air before use. Fig. 2 shows the transient I_{SC} variations of batteries with untreated and pre-wetted cellophane films. Both batteries have similar trends for increasing I_{SC} before 300 s, indicating that the motion of water in both batteries is nearly the same at this stage. After 300 s, however, the battery with an untreated membrane attained a maximum current 0.4 mA as a plateau, possibly due to the slow water absorption process of the untreated cellophane film. But I_{SC} of the pre-wetted membrane battery increased to 1.1 mA, ~2.75 times as large as the one with an untreated cellophane film. The larger maximum I_{SC} with pre-wetted films verifies the more rapid ionic exchange rate in the larger pores, as stated previously. To maximize the power output for LED or electrophoretic devices, pre-wetted cellophane films were thus used in all batteries discussed in the following sections.

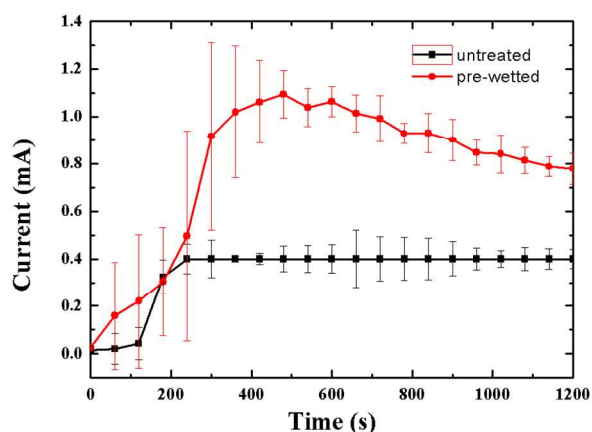


Fig. 2 Comparison of closed circuit current I_{SC} from fluidic batteries with untreated and pre-wetted cellophane films. The pre-wetted cellophane film was prepared by soaking in deionized water for 5 minutes and dried in air overnight. The error bars show the maximum deviations of measurements from 5 individual batteries.

Origami designs for multiple galvanic cells

(a) Repetition of single-cell designs

To produce a battery of multiple cells, one can print multiple copies of the one-cell pattern on one paper and fold them into a pack of single-cell batteries; an example is given in Fig. S3. Two single-cell patterns of mirror symmetry were printed on a filter paper; with a similar folding procedure, one can easily produce a battery with two cells in series. If the two single-cell patterns are printed in parallel, one can fold them into two cells in parallel. Through these demonstrations, the origami skill shows a great potential to integrate multiple planar designs into a single three-dimensional device.

(b) Designs for multiple cells

Besides assembly with multiple copies, with proper origami pattern designs one can also pack multiple cells in series or parallel into a single folded battery. The designs are shown in Fig. S1 with the folding sequences in Fig. S4-7. As these figures show, the design principle in this work follows a simple folding procedure so that users can easily assemble a battery quickly. Generally, the multiple-cell batteries all possess six pieces of papers with fluidic patterns. The folding sequences

are nearly the same except for varied size of cellophane films and electrodes. The usage of cellophane films instead of a salt bridge makes the assembly simpler and quicker. In general, one can fold a battery manually within two minutes. The designs for 2, 4, 6 and 8 cells presented in the ESI are discussed in the following sections.

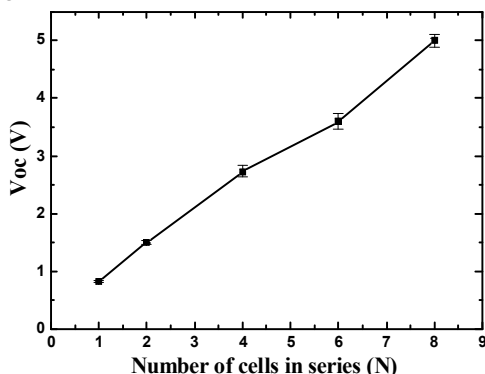


Fig. 3 Variation of V_{OC} with number of cells in prepared batteries. The V_{OC} values were recorded 300 seconds later after 30 μL of water was added into the paper-based batteries. The error bars show the maximum deviations of measurements from 5 individual batteries.

Electric performance of fluidic batteries

Open-circuit voltages of origami fluidic batteries were first identified to test the available electric potential from the batteries. Fig. 3 shows the variation of V_{OC} with the number of galvanic cells in series. In the paper-based batteries, the cell resistance is typically larger than in normal galvanic batteries because of the small rates of ionic exchange in fibrous fluidic channels, leading to V_{OC} much smaller than the theoretical values. As shown previously, an averaged $V_{OC} = 0.82$ V, or 41 % of the theoretical value, was observed for single-cell batteries. The resistance increased as the number of galvanic cells increased, resulting in increased fractional loss of voltage in multiple-cell batteries: 1.50 V for two cells, 2.73 V for four cells, 3.61 V for six cells and 4.90 V for eight-cell structures. The voltage output is roughly fitted in a linear relation as

$$V_{OC} = 0.8 + 0.5 N \quad (4)$$

in which N is the number of galvanic cells in series.

The origami paper-based fluidic batteries provide fairly stable power output for at least 20 min. Fig. 4 (a) shows the temporal evolution of V_{OC} from batteries of various designs. The varying values of V_{OC} at time=0 for each battery is possibly due to the time delay between electrical measurements and water addition. Nonetheless, for all batteries, an initial induction period 100 s after water addition is needed for the fluidic batteries to attain a stable potential output. This induction period is likely attributed to the wetting interval for water to pass through all fluidic channels and to create stable conductive connections between the two galvanic electrodes. After the fluidic connections are well developed, these fluidic batteries made with the origami technique showed stable output voltage for at least 20 min.

The current responses, however, show a larger induction period than that of the voltage output (Fig. 4(b)). For a single-cell battery, I_{SC} increased slowly and attained 1 mA after 300 s. This longer induction period (< 100 s for voltage response) is possibly caused by the fact that the current output requires not only the wetting interval but also that for ionic diffusion in the cellophane films. Nevertheless, the current remains above 1

mA for approximately 5 min and begins to decay, indicating gradual decrease of concentration of Cu^{2+} in the electrolyte layers.²⁶ A total decay period ~ 2 h is needed for the battery to attenuate completely. I_{SC} of all other multi-cell batteries follows a similar trend. Because smaller cellophane films are used when more cells are connected in series (see Table S1 for details), the induction period is, however, smaller (< 200 s) to achieve the maximum I_{SC} . Moreover, the smaller ion-exchange area in cellophane also produces a smaller current output, or maximum I_{SC} .

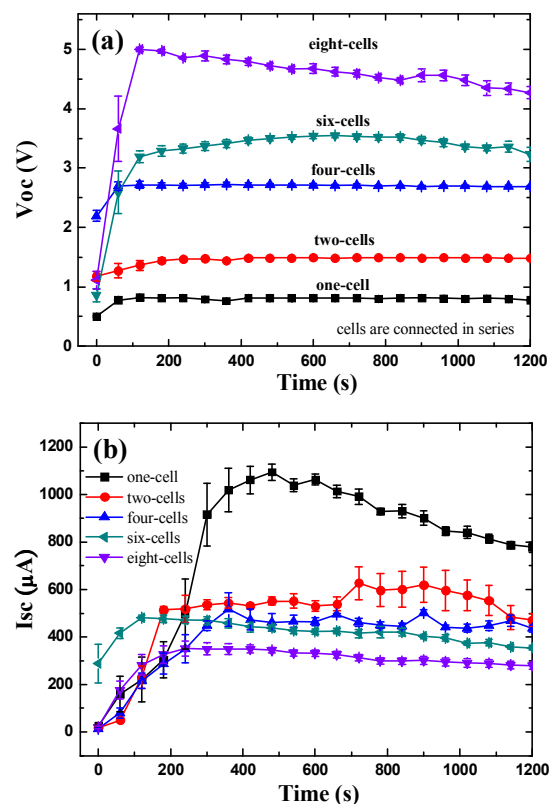


Fig. 4 (a) Transient profiles of V_{OC} after water added into the paper-based batteries. The error bars show the maximum deviations of measurements from 5 individual batteries. (b) Transient profile of I_{SC} after water addition. The number of cells in series is indicated in the figure.

Packing into a power bank for long-term usage

The prepared fluidic batteries can provide sufficient power for electric devices with a requirement of a small energy density. To understand the electric capacity of the fluidic battery, we connected a LED to release the energy from the battery. A battery of four-cell design (~ 2.73 V) can regularly provide sufficient power for a red LED lamp, as shown in Fig. 5, for 65 min, but, under regular discharging conditions in the laboratory, water evaporation from paper-based batteries decreased the power output, which was observed from a dimmer LED after using the battery for 20 to 30 min. The dried battery can be reused again with reasonable power output to light the LED until the chemicals are totally consumed. However, if one needs to operate a device for more than 20 min, it is necessary to supply water intermittently (~ 10 μL every 20 min in our case) to prevent the batteries from drying. To save the manual labour for the water addition, one can also keep the fluidic battery in water. If the battery is soaked in water, it disintegrates, however, after about 20 min because of the poor

Lab on a Chip

adhesion of the glue. A wax-coating method was then developed to prevent the battery from falling apart after soaking. As shown in Fig. 6, a paper-based battery was first dipped into melting wax to create a protective layer. The water inlet was covered intentionally during the wax-dipping to prevent the fluidic channels from clogging. The wax coating provided a strong protective layer so that the battery could stay in water without falling apart. The wax-coated batteries were then half submerged in a small plastic cabinet filled with water (Fig. 7(a)) to form a portable power bank for prolonged usage. The water level was just high enough to reach the water inlet of the batteries. With this setup, the water kept saturating the fluidic channels in the battery, and a four-cell battery could drive the LED for over 65 min without added water. Moreover, one can also put two four-cell batteries in series (~ 5 V) to drive LED continuously for more than five hours (Fig. 7(b)). This device can help providing necessary electric power for diagnostic devices in resource-limited area with little amount of clear water at moderate pH level.

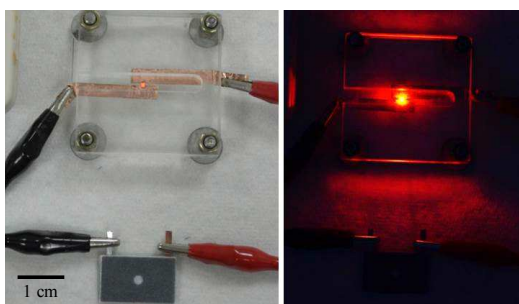


Fig. 5 A four-cell in series structure paper-based fluidic battery (~ 2.73 V) connect with a red LED lamp. The battery provides sufficient power for the LED for 65 minutes. The right side picture is taken in dark situation.

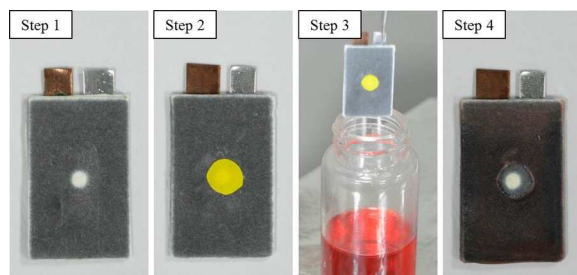


Fig. 6 Wax coating process for waterproof battery to prevent the battery from falling apart after soaking. The water inlet was taped, and then the battery was dipped into melting wax. After wax coatings solidify, the waterproof battery is finished. The water inlet is permeable to water while the rest of the parts are completely waterproof.

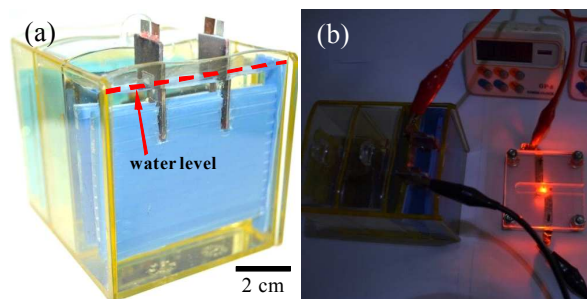


Fig. 7 Paper-based power bank is reformed from a plastic cabinet. Two plastic plates with small slit are put in the space to help the batteries held in position when the power bank operates. (b) The power bank with two wax

coated batteries (each has 4-cell in series) can light the LED for hours, which suggests the success of wax coating process in Fig. 6 in making waterproof batteries.

Power supply for electrophoretic devices

Among many diagnostic or analytical applications, the separation of chemicals is of great importance and readily achievable with electrophoresis, but traditional electrophoretic devices are generally large and require bulky external power supplies to achieve high-voltage electrophoresis (> 20 V cm^{-1})²⁷. To miniaturize traditional electrophoretic devices for point-of-care services, we fabricated a self-powered microfluidic device to demonstrate the possibility of paper-based devices for inexpensive separation of chemicals.

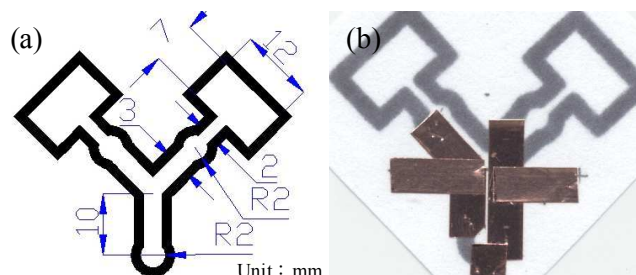


Fig. 8 (a) The design of the Y-shaped paper-based channel, and (b) the patterns of copper tapes around the channel to help separating MB.



Fig. 9 Electrophoresis in Y-shaped channels with 3 paper-based batteries. Each battery used here contains 4 galvanic cells, and were connected in series to provide electric potential of ~ 8 V. 20 μL MB solution was dripped in the circular reservoir at the bottom. The electric field (estimated to be ~ 40 V/cm across the channel) drives the anionic MB molecules toward the cathode, leading to solute enrichment on the right hand side of the channel and the MB flow into only one of the two split channels. The total time to wet the channels is about 2 minutes.

The electrophoretic effects on paper were first demonstrated on separating methylene blue (MB) solution with a regular external power supply (Fig. S8). A Y-shaped channel (width 5 mm) was cut from a piece of a regular filter paper; several pieces of copper tape were attached to create electrodes for electrophoresis. Because MB is cationic, the molecules are repelled by the anode and move toward the cathode. As shown in Fig. S8, when an electric field greater than 30 V cm^{-1} is provided, the electrophoretic force becomes strong enough to redirect the MB molecules towards one branching channel.

To combine the electrophoretic device with fluidic batteries, a smaller version Y-shaped channel (Fig. 8(a)) was designed; patterns of copper tape were attached around the fluidic channels (Fig. 8 (b)) to generate an electric field. The electrodes on the Y-shaped channels were then connected to three 4-cell

fluidic batteries in series, which provided potential 8 V for the device throughout the whole electrophoretic process. Because the width is small (2 mm), an electric field 40 V cm^{-1} , greater than the minimum 30 V cm^{-1} determined previously for MB separation, was generated. As Fig. 9 shows, the combination of the battery with electrophoretic devices resulted in a one-directional motion of MB; the cationic MB molecules moved toward the cathode with a significant concentration effect. Similar results can also be obtained for anionic compounds, such as Congo red, by simply switch the polarity of electrodes. This electrophoretic device combined with the fluidic battery shows the potential of using paper-based devices in separation of charged bio-molecules.

Conclusion

We developed a new approach to fabricate 3-D fluidic batteries with an origami principle. The fluidic channels were fabricated with a commercial wax printer following with a heating process. Metal electrodes and cellophane films were glued onto the printed patterns and then folded into three-dimensional structures to form a single battery. Two half reactions (Al/Al^{3+} and Cu/Cu^{2+}) in the folded single-cell battery provided an open-circuit potential 0.82 V. Batteries of five designs were created in this work to generate multiple-cell batteries. The open circuit voltage V_{OC} varied from 0.87 V for a single-cell to 4.90 V for an eight-cell battery. All multi-cell batteries attained a stable power output in less than 100 s after water was added to the battery, and maintained a stable V_{OC} and closed-circuit current I_{SC} for at least 20 min. A wax-dipping process was developed to create a protective layer around the battery so that the battery can be soaked in water to avoid intermittent manual addition of water. The fabricated battery can provide sufficient power for regular devices, such as LED lamps, for hours. Furthermore, a paper-based device utilizing a Y-shaped channel was fabricated to show the capability of electrophoretic separation on paper. After connection to the fluidic battery, an electric field 40 V cm^{-1} was generated to separate cationic methylene blue molecules, and redirected the fluid motion to form streams with and without MB molecules. In summary, this work shows a rapid assembly of a fluidic battery and opens an avenue for prospective applications in printed electronic devices for biomedical analysis.

Acknowledgement

National Science Council in Taiwan supported this research through Grants NSC 102-2221-E-002-080 and NSC 101-2221-E-002-177-MY2.

Notes and references

^a No. 1, Sec. 4, Roosevelt Road, Taipei, 10617 Taiwan. Department of Mechanical Engineering, National Taiwan University; E-mail: jtyang@ntu.edu.tw

^b No. 1, Sec. 4, Roosevelt Road, Taipei, 10617 Taiwan. Department of Chemical Engineering, National Taiwan University, Taiwan; E-mail: liaoy@ntu.edu.tw

† Electronic Supplementary Information (ESI) available: folding of two-cell, four-cell, six-cell and eight-cell batteries. See DOI: 10.1039/b000000x/

- 1 L. Nyholm, G. Nystrom, A. Mihranyan and M. Stromme, *Adv. Mater.*, 2011, **23**, 3751-3769.
- 2 G. Nystrom, A. Razaq, M. Stromme, L. Nyholm and A. Mihranyan, *Nano Lett.*, 2009, **9**, 3635-3639.

- 3 L. Y. Yuan, X. Xiao, T. P. Ding, J. W. Zhong, X. H. Zhang, Y. Shen, B. Hu, Y. H. Huang, J. Zhou and Z. L. Wang, *Angew. Chem.-Int. Edit.*, 2012, **51**, 4934-4938.
- 4 G. Y. Zheng, L. B. Hu, H. Wu, X. Xie and Y. Cui, *Energy Environ. Sci.*, 2011, **4**, 3368-3373.
- 5 M. Hilder, B. Winther-Jensen and N. B. Clark, *J. Power Sources*, 2009, **194**, 1135-1141.
- 6 H. Liu and R. M. Crooks, *Analytical Chemistry*, 2012, **84**, 2528-2532.
- 7 S. W. Wang, L. Ge, Y. Zhang, X. R. Song, N. Q. Li, S. G. Ge and J. H. Yu, *Lab on a Chip*, 2012, **12**, 4489-4498.
- 8 N. K. Thom, K. Yeung, M. B. Pillion and S. T. Phillips, *Lab on a Chip*, 2012, **12**, 1768-1770.
- 9 A. W. Martinez, S. T. Phillips and G. M. Whitesides, *Proc. Natl. Acad. Sci. U. S. A.*, 2008, **105**, 19606-19611.
- 10 A. W. Martinez, S. T. Phillips, M. J. Butte and G. M. Whitesides, *Angew. Chem.-Int. Edit.*, 2007, **46**, 1318-1320.
- 11 A. W. Martinez, S. T. Phillips, B. J. Wiley, M. Gupta and G. M. Whitesides, *Lab on a Chip*, 2008, **8**, 2146-2150.
- 12 A. W. Martinez, S. T. Phillips and G. M. Whitesides, *Proceedings of the National Academy of Sciences USA*, 2008, **105**, 19606.
- 13 D. A. Bruzewicz, M. Reches and G. M. Whitesides, *Anal. Chem.*, 2008, **80**, 3387-3392.
- 14 W. Dungchai, O. Chailapakul and C. S. Henry, *Analyst*, 2010, **136**, 77-82.
- 15 A. Nilghaz, D. H. B. Wicaksono, D. Gustiono, F. A. A. Majid, E. Supriyanto and M. R. A. Kadir, *Lab on a Chip*, 2011, **12**, 209-218.
- 16 E. Carrilho, A. W. Martinez and G. M. Whitesides, *Anal. Chem.*, 2009, **81**, 7091-7095.
- 17 G. G. Lewis, M. J. DiTucci, M. S. Baker and S. T. Phillips, *Lab on a Chip*, 2012, **12**, 2630-2633.
- 18 H. Liu, Y. Xiang, Y. Lu and R. M. Crooks, *Angew. Chem.-Int. Edit.*, 2012, **51**, 6925-6928.
- 19 J. M. Chen, M. C. Kuo and C. P. Liu, *Jpn J Appl Phys*, 2011, **50**.
- 20 A. V. Govindarajan, S. Ramachandran, G. D. Vigil, P. Yager and K. F. Bohringer, *Lab on a Chip*, 2012, **12**, 174-181.
- 21 L. Ge, S. M. Wang, X. R. Song, S. G. Ge and J. H. Yu, *Lab on a Chip*, 2012, **12**, 3150-3158.
- 22 J. X. Yan, M. Yan, L. Ge, J. H. Yu, S. G. Ge and J. D. Huang, *Chemical Communications*, 2013, **49**, 1383-1385.
- 23 N. K. Thom, K. Yeung, M. B. Pillion and S. T. Phillips, *Lab Chip*, 2012, **12**, 1768-1770.
- 24 N. K. Thom, G. G. Lewis, M. J. DiTucci and S. T. Phillips, *RSC Advances*, 2013, **3**, 6888-6895.
- 25 X. W. Zhang, J. Li, C. G. Chen, B. H. Lou, L. L. Zhang and E. K. Wang, *Chemical Communications*, 2013, **49**, 3866-3868.
- 26 N. Thom, G. G. Lewis, M. DiTucci and S. Phillips, *RSC Advances*, 2013.
- 27 Z. Deyl, *SEPARATION METHODS*, Elsevier Amsterdam Netherlands, 2011.